Dynamic Delamination Propagation in Composite Beams

BHAVANI V. SANKAR AND SHOUFENG HU
Department of Aerospace Engineering, Mechanics & Engineering Science
University of Florida
Gainesville, FL 32611

(Received May 17, 1990)
(Revised November 5, 1990)

ABSTRACT: The problem of dynamic delamination growth in composite beams is analyzed using finite element method. The delaminated beam is modeled as two beams above and below the plane of delamination. Spring elements are used to connect the beams in the uncracked portion. The dynamic energy release rate is calculated from the strain energy in the crack-tip springs. The crack is allowed to propagate when the energy release rate reaches a critical value estimated from experiments. The crack growth histories are compared with results from tests on composite beams containing implanted delaminations. The finite element model is found to be adequate in predicting dynamic delamination growth in laminated composite beams.

KEY WORDS: delamination, dynamic fracture, finite elements, impact damage.

INTRODUCTION

FIBER COMPOSITES ARE mostly used in the form of laminates, which are susceptible to delamination during fabrication or service. A delamination may propagate under static, fatigue or dynamic loads for which the structure is designed, as well as due to dynamic loads caused by unexpected impact events. Environmental factors such as temperature may also increase the chance of delamination growth. Frequent nondestructive inspection of composite structures can be expensive, hence it may be necessary to allow for the existence of some delamination type cracks in the structural design. The objective of this study is to develop a simple finite element procedure for modeling delaminations in laminated composite beams, and to predict their growth in dynamic loading environments. The model is verified by comparing with some available experimental data, and also by performing impact tests on laminated beams with implanted delaminations.

Dynamic fracture is still considered a formidable problem because computation of appropriate dynamic fracture parameters such as stress intensity factor (K), dynamic energy release rate (G), or the elastodynamic path independent

0021-9983/91/11 1414-13 $6.00/0

integral (J') is very difficult due to the inertial and stress wave effects, and measuring the critical values of those parameters as a function of crack velocity is not a trivial experimental task. A general discussion of the mechanics of dynamic crack growth, various analytical methods of evaluating dynamic crack parameters, and a review of numerical methods can be found in Reference [1]. Grady and Sun [2] performed impact tests on graphite/epoxy beams with implanted delaminations. The delamination crack propagation was recorded using a high-speed camera. The crack-tip position, and hence the crack velocity, was measured as a function of time. Plane finite elements were used in the analysis, and the energy release rate was computed using the crack closure integral method. The analysis results were used to predict the critical energy release rate for the initiation of delamination propagation.

Kanninen [3,4] has developed various elastic foundation spring models for dynamic analysis of unstable crack propagation and arrest in DCB specimens. The advantage of the method lies in its simplicity in computing energy release rate as a function of time. The difficulty is in evaluating suitable foundation parameters for orthotropic as well as laminated composite materials.

Numerical methods based on finite elements and finite differences have been found to be very convenient in the analysis of brittle dynamic fracture of structures of complicated geometries [5,6]. The advantages of numerical methods are: crack propagation can be simulated by releasing the crack tip nodes gradually; singular crack tip elements can be used to improve the accuracy of stress intensity factors; and path independent integrals can be easily evaluated. Farris and Doyle [7] used the wave-guide analysis for a beam containing a finite crack. They used the zero-volume path independent integral to compute the dynamic J', and the stress intensity factors. The accuracy of the approach was demonstrated by comparing with the two dimensional analysis.

In the present study finite elements are used to compute the dynamic energy release rate in a laminated composite beam. A beam element with nodes offset to one side, either top or bottom, is used to model the two portions of the beam above and below the plane of delamination. The offset beam element has the advantage of allowing crack propagation without renumbering the nodes, and more importantly, is convenient in modeling the partial contact and slip at the delamination interface. The top and bottom portions of the beam can be con-

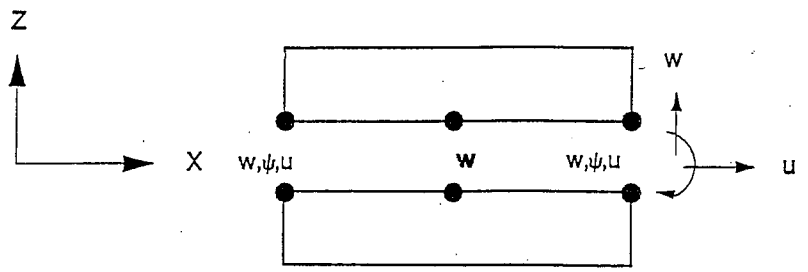

Figure 1. *Beam finite element with offset nodes.*

nected either by foundation springs or rigid elements as will be described below. The energy release rate has been calculated using three different methods: (1) zero-volume J'-integral; (2) a crack closure method for beams; and (3) the strain energy in the crack-tip springs. The crack propagation can be studied using a fracture criteria, such as $G = G_c$ for crack growth, where the critical strain energy release rate G_c has to be measured from suitable experiments. The following sections describe the development of a composite beam finite element, its application in the analysis of dynamic delamination propagation, and experiments to verify the numerical model.

FINITE ELEMENT MODEL

The beam element used in the present study (Figure 1) has three nodes. The two extreme nodes have three degrees of freedom each, u, w and ψ, which are the axial displacement, transverse displacement and rotation about the y-axis, respectively. The central node is assigned w degree of freedom only. Thus the variation of w-displacements are quadratic, whereas u and ψ vary linearly. The displacements are interpolated as

$$w(x) = w_1 N_1(x) + w_2 N_2(x) + w_3 N_3(x) \tag{1}$$

$$u(x) = u_1 N_4(x) + u_2 N_5(x) \tag{2}$$

$$\psi(x) = \psi_1 N_4(x) + \psi_2 N_5(x) \tag{3}$$

where $N_1(x) = (1 - 2x')\ (1 - x')$, $N_2(x) = 4x'(1 - x')$, $N_3(x) = x'(2x' - 1)$, $N_4 = (1 - x')$, $N_5 = x'$, $x' = x/L$, and L is the element length. The equations of motion for the laminated beam are:

$$\varkappa b A_{55} \frac{d}{dx}\left(\frac{dw}{dx} + \psi\right) + p(x) = 0 \tag{4}$$

$$bD_{11}\frac{d^2}{dx^2}\psi - \varkappa b A_{55}\left(\frac{dw}{dx} + \psi\right) \pm bA_{11}\frac{h}{2}\frac{d^2}{dx^2}\left(u \pm \frac{h\psi}{2}\right) = 0 \tag{5}$$

$$bA_{11}\frac{d^2}{dx^2}\left(u \pm \frac{h\psi}{2}\right) + t(x) = 0 \tag{6}$$

In the above equations, b and h are the beam width and thickness, $p(x)$ and $t(x)$ are the distributed transverse and axial forces acting on the beam, and the $\pm$ signs correspond to beams with nodes offset to bottom and top side respectively. A_{11}, A_{55} and D_{11} are conventional laminate stiffness coefficients, and $\varkappa$ is the shear correction factor. It is assumed that there is no extension-twisting or bending-twisting coupling in the laminate.

The stiffness and mass matrices can be derived by using the Galerkin method. The non-zero elements of the stiffness and mass matrices are given in the Appen-

dix. It should be noted that some of the terms in the stiffness and mass matrices are different for the top and bottom elements. In the Appendix they are denoted by a $\pm$ sign. If we add the stiffness or mass matrices of the top and bottom elements, we recover the corresponding matrices of a conventional beam element with nodes at the midplane. In some applications the middle node can be eliminated by static condensation, and we will have 6×6 stiffness and mass matrices [8,9].

The performance of the offset beam element was evaluated by considering several static and dynamic problems. In the dynamic case, both free vibration and transient problems were considered. In spite of the fact that exact integration was used in computing the stiffness matrix, there was no shear locking, because of the choice of different order of interpolation functions used for transverse displacement, axial displacement and rotation. The details of the derivation of the stiffness and mass matrices, and evaluation of the offset beam finite element can be found in [10].

MODELING DELAMINATIONS

In modeling dynamic crack problems we will assume that there is a single dominant delamination crack in the beam, and also the crack will propagate in a self-similar manner. Thus possibilities of crack branching are ignored in the present study. Experimental studies [2] indicate that this is a valid assumption. We will assume brittle fracture behavior, and use the principles of linear elastic fracture mechanics in the analysis. The beam can be assumed to be made up of two sublaminates one above and the other below the plane of delaminations. The top portion above the plane of delamination is modeled by elements with nodes offset to the bottom side, and the bottom portion by elements with nodes at the top. In order to connect the top and bottom portions, two types of connecting elements are used. In the first approach, three spring elements, a transverse spring (k_w), an axial spring (k_u), and a torsional spring (k_ψ), are used to connect the extreme nodes. The middle node in an element is connected to a transverse spring only. The stiffness matrix of a spring element, for example transverse spring, is of the form

$$[k] = \begin{bmatrix} k_w & -k_w \\ -k_w & k_w \end{bmatrix}; \begin{Bmatrix} w_1 \\ w_2 \end{Bmatrix} \tag{7}$$

In the second approach the top and bottom portions of the beam were connected by a rigid element that ensures continuity of transverse displacement, axial displacement and rotation. Alternatively one can have common nodes in the undelaminated portion. This is equivalent to using a single beam element in the uncracked portion. The rigid element connection is convenient in modeling static crack problems or dynamic problems with stationary cracks, as the energy release rate can be directly computed from the forces transmitted by the crack-tip rigid element [8,9]. A gap element was used in the delaminated portion to monitor contact between delaminated surfaces. In the examples considered contact

forces between the sublaminates were found to be very small, and hence frictional forces between delaminations were neglected.

In the present study energy release rate is used as the crack propagation criterion. For a dynamic problem this can be expressed as [4]

$$G = \frac{d}{dA}(W - U - T) \tag{8}$$

where W, U, and T are work done by external loads, elastic strain energy, and kinetic energy in the beam respectively, and A is the area of the crack surface. Three methods were used to compute energy release rate. In the case of spring model, the energy release rate is simply the sum of strain energies per unit length in the crack-tip springs [10]. This can be calculated from the differences in the displacements and rotation of the top and bottom nodes at the crack tip and the spring constants k_w, k_u and k_ψ. The other two methods pertain to the rigid element connection at the crack-tip. The second method is the zero-volume path integral [7], which is a function of the bending moment, shear and axial force resultants in the sublaminates attached to the crack-tip [8,9]. This can be written as

$$G = U^{(1)} + U^{(4)} - U^{(2)} - U^{(3)} \tag{9}$$

where $U^{(i)}$ is the strain energy per unit length in the ith sublaminate connected to the crack-tip (see Figure 2). The third method is a crack closure technique developed for offset beam finite elements [8–10]. This is similar to the conventional crack closure method, except now the nodal forces are the bending moment, transverse force and shear force transmitted by the rigid element at the crack tip node. The strain energy released is half the work done by these forces through the differences in rotation and displacements of nodes behind the crack tip. It can be shown that the zero-volume path integral and crack closure methods give identical results for energy release rate [8–10].

It should be noted that all the three methods are good for static problems as well as dynamic problems with stationary cracks. For moving crack problems one has to use only the spring model for the following reasons. In the case of spring model, the crack growth is simulated by breaking the crack-tip springs. Thus the strain energy stored in the spring, which is equivalent to the energy required to create new crack surfaces, will be removed from the system, and hence the energy balance as given by Reference [8] will be satisfied. When using 2-d and 3-d models for a moving crack problem the singularity at the crack-tip provides the necessary mechanism for energy dissipation. Whereas beam and plate type elements do not possess singular behavior, and there is a need for an explicit energy dissipation mechanism. In this context, the springs used in the present model can be considered as cohesive springs or elastic springs that represent a thin layer of epoxy in between the layers. The results for G were not very sensitive to the spring constants as long as they are sufficiently stiff [10]. The choice of appropriate spring constants for laminated composite materials requires fur-

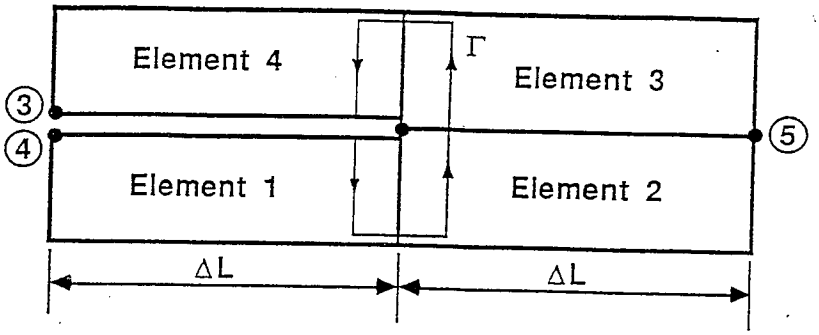

Figure 2. *Crack-tip elements for zero-volume path integral.*

ther studies. In the present study the spring constants were selected by trial and error such that the value of G computed is equal to that obtained from the zero-volume path integral method. The foundation spring constants used by Kanninen [3] provided a good starting value for the trial and error procedure.

NUMERICAL EXAMPLES

The proposed finite element model was verified by considering the example given in Reference [2]. The beam properties, dimensions and loading are given below for the sake of completion. A 20 ply $[90,0]_s$ graphite/epoxy laminate is modeled as a homogeneous orthotropic beam with elastic constants $E_1 = E_2 = 72.4$ Gpa, $E_3 = 10.3$ GPa, $G_{12} = 5.0$ GPa, $\nu_{13} = \nu_{23} = 0.33$, $\nu_{12} = 0.025$, and mass density $\varrho = 1.58 \times 10^{-5}$ N-s^2/cm^4. The beam dimensions are $173 \times 25 \times 2.5$ mm. The beam is fixed at one end and the other end is free. The initial delamination is 25.4 mm long and its center is at 102 mm from the fixed end. The delamination is at the midplane of the beam. The impact force is applied at a point 130 mm from the fixed end. The impact force is taken as [2]

$$F(t) = 1530 \sin(\pi t/125\ \mu s)N,\ 0 < t < 125\ \mu s$$

$$= 0,\ t > 125\ \mu s$$

The flexural deflection at the left crack tip for the above example obtained using the present method is plotted in Figure 3. The agreement with the result of Reference [2] is very good. The strain energy release rate was computed using the three methods described earlier, and they are shown in Figure 4. It was found [10] that the energy release rate G did not vary very much with the spring constants k_w and k_ψ. This indicates that Mode II behavior is dominant in the present problem. The results in Figure 4 were obtained with $k_u = 0.8G_{12}bL/h$, where L, b, and h are the length, width and thickness of the crack tip sublaminates. It may be seen that all the three methods provide the same G history for this stationary crack problem.

DYNAMIC CRACK PROPAGATION–COMPARISON WITH EXPERIMENTS

The crack propagation is assumed to occur when G equals the critical value G_c. In the finite element model crack propagation is simulated by breaking the crack-tip springs when $G = G_c$. The stiffness matrix has to be modified for subsequent time steps. The average velocity of crack propagation is found by considering the crack advance over several time steps. Although G_c has been assumed to be a constant material property in the present study, in general crack resistance increases with velocity [4]. In that case an iterative procedure has to be used since the crack velocity is not known apriori. An estimated G_c value has to be chosen based on the average velocity assuming the crack will propagate to the next node. If the calculated G is less than G_c, then the crack propagation will not have occurred.

The above described method was used to predict delamination propagation of a test specimen given in Reference [2]. The dimensions and properties of the beam were described in the previous section. The critical energy release rate was assumed to be 350N/m as given in [2]. Comparison of experimental result and present finite element prediction are shown in Figure 5. It is interesting to note

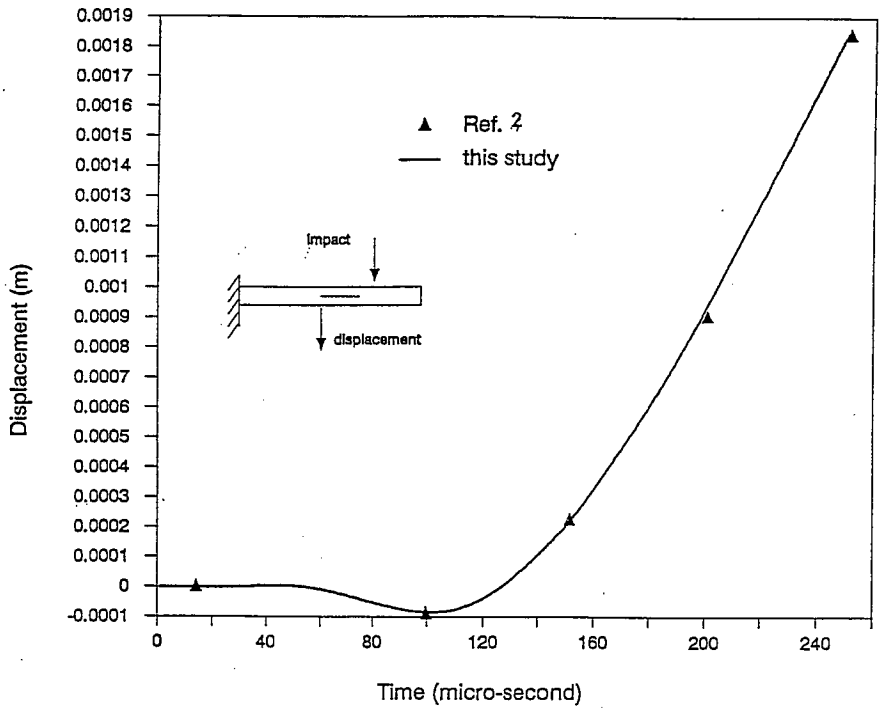

Figure 3. *Comparison of beam deflection.*

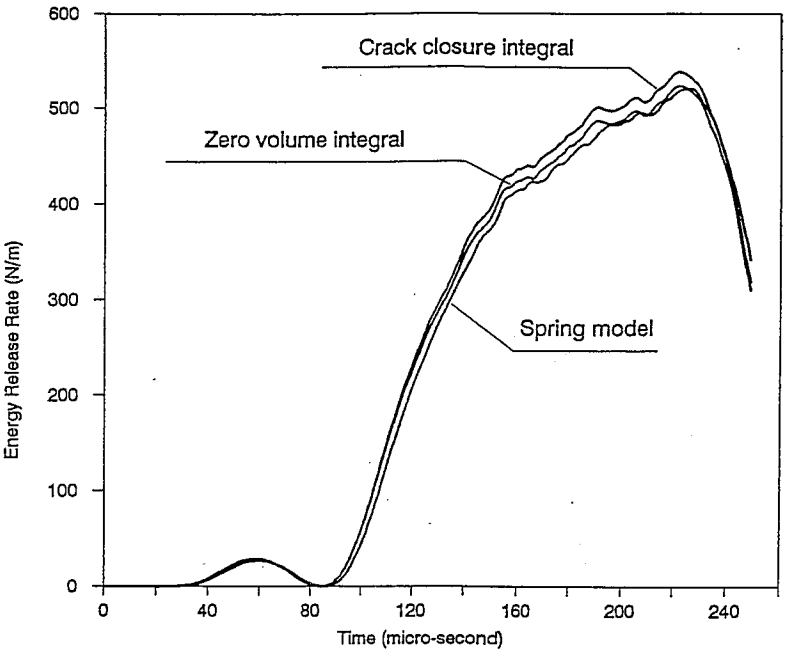

Figure 4. *Energy release rate history from various methods.*

that the finite element model is able to predict the intermittent crack arrest during 400 μs $< t <$ 600 μs. The discrepancies in results after about 700 μs can be attributed to the fact that we have not accounted for increased crack resistance at higher velocities. That is why the numerical model predicts a higher velocity than the experimental results.

A second set of evaluations of the model was done by performing pendulum impact tests on glass/epoxy beam with implanted delaminations. The description of the impact pendulum can be found in Reference [11]. The total mass of the impact tup was 13.84 kg. A 6.25 mm diameter steel impactor nose was used. The impact velocity, rebound velocity and impact force history were recorded using electronic data acquisition systems. All specimens were cut from a 300 $\times$ 300 mm $[0/90/90/0]_{4s}$ glass/epoxy plate cured in the autoclave. The properties of the material were: $E_1 = 37$ GPa, $E_2 = 11.54$ GPa, $G_{12} = 3.46$ GPa, $\nu_{12} = 0.285$, $\varrho = 1930$ kg/m^3. The specimen dimensions and location of delamination are shown in Figure 6. The delamination was created by inserting a teflon strip in the prepregs before curing. The specimen overhang on either side of the supports was designed to be unequal to cause preferential crack extension to one side. A soft rubber padding was placed on the specimen at the impact point to minimize local indentation damage.

The experimental results for six impact tests are presented in Table 1. The results include impact and rebound velocities, maximum impact force, impact

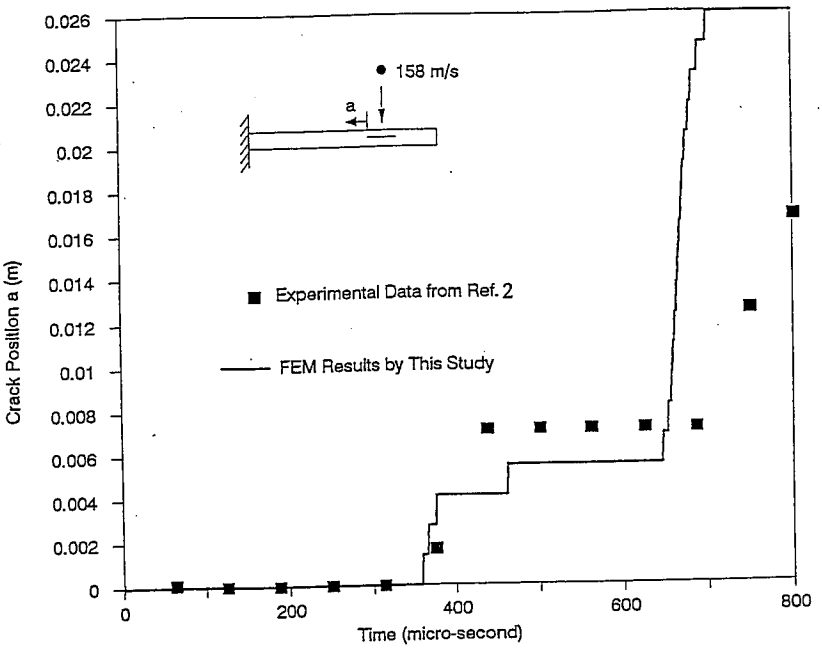

Figure 5. *Comparison of crack growth history.*

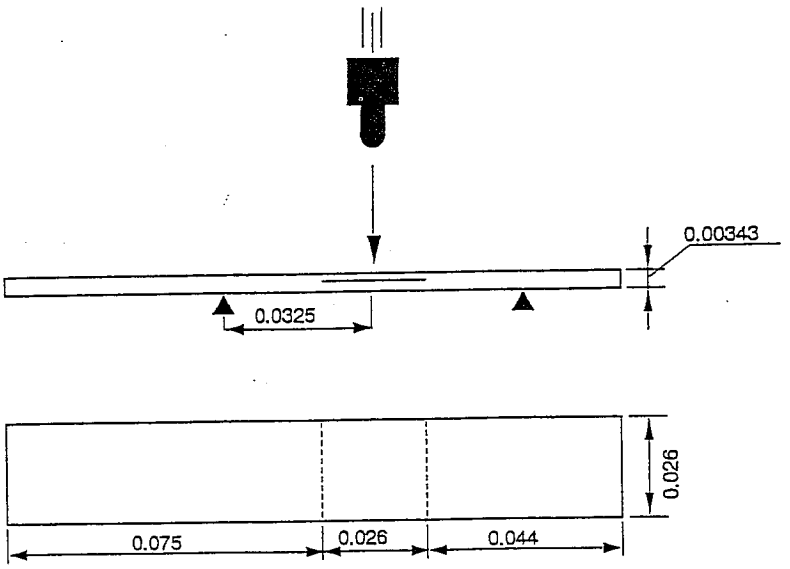

Unit: m

Figure 6. *Beam used in impact tests (dimensions in meter).*

Table 1. Impact test results.

Specimen No.	Impact/Rebound Velocity (m/s)	Max. Impact Force (N)	Impact Duration (ms)	Left/Right Crack Extension (mm)
1	0.88/0.79	2060	32.26	69.6/2.4
2	0.99/0.69	1943	29.42	57.3/1.0
3	0.97/0.68	1926	29.56	57.3/1.2
4	0.94/0.66	1815	29.36	52.5/0.5
5	1.00/0.76	1677	30.87	54.9/1.6
6	0.95/0.62	2031	28.30	56.5/0.5

duration, extension of left and right crack tips. Sample impact force histories from two impacts are shown in Figure 7. One of them is for a specimen in which crack propagation did not occur.

The finite element model was used to predict crack extension in the test specimens. The beam was modeled by 580 offset beam elements. The element length in the vicinity of crack tips was 0.5 mm. The time step for Newmark integration was 1 μs. The impact velocity was 0.97 m/s corresponding to that of Specimen 3 in Table 1. The experimentally measured impact force history was applied to the

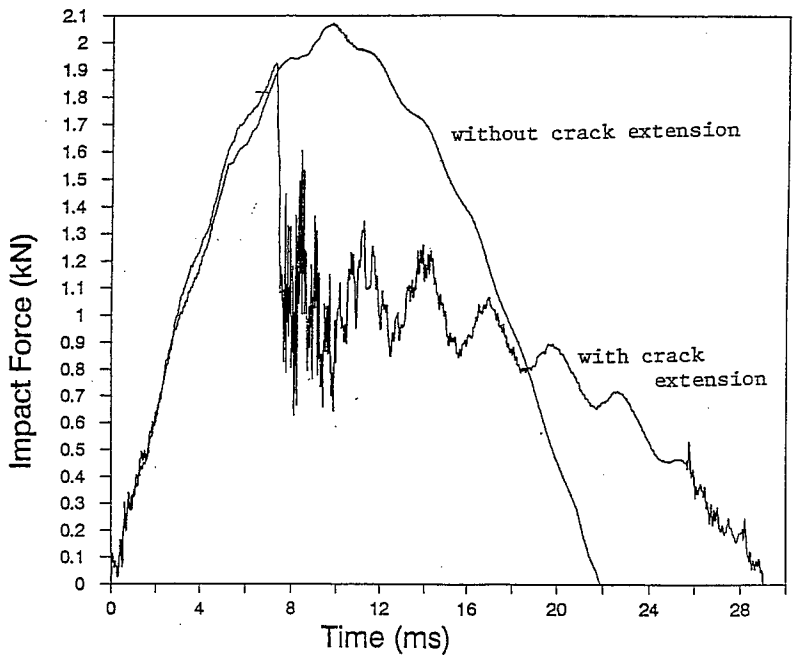

Figure 7. *Impact force in beams with and without crack extension.*

model. The history corresponded to that of the failed specimen in Figure 7. The G_c value was taken as that computed at a time just before the load drop observed in the impact test. The predicted crack extension history is shown in Figure 8. From the results the crack extensions were 61 mm and 3 mm at the left and right crack-tips respectively. Corresponding test results were 57.3 mm and 1.2 mm (see Table 1). Thus the present finite element model is able to predict the final position of the crack from the initial delamination description and load history.

Although the experimental impact force history was used in the numerical simulation, the impact force history can be computed by having a nonlinear contact spring at the impact point. This step is important for developing a numerical capability to predict crack growth in composite structures. Because of the nonlinear contact springs, an iterative procedure has to be used in computing the impact force at each time step [12]. When the impact mass is much larger, and the target is more flexible than the contact spring, a simple spring-mass model can be used to predict the maximum impact force and duration [2,10]. Then, the sinusoidal impact force history can be applied to the finite element model to compute G. If G_c is known, then at least initiation of crack propagation can be predicted. This will be a useful design tool in estimating damage tolerance of composite structures with known delaminations. This approach was used to predict the impact force history for the beam shown in Figure 6, when delamination does

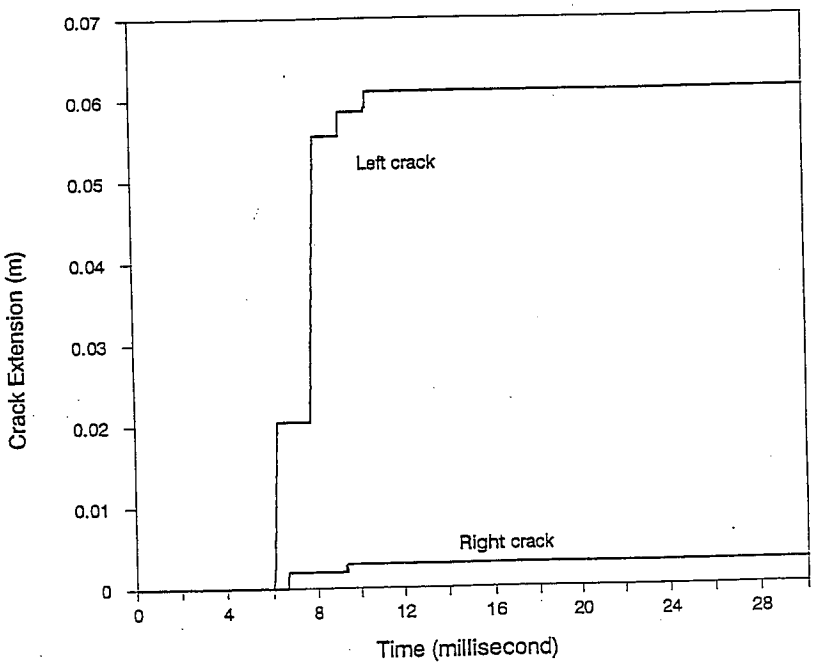

Figure 8. *Predicted crack growth history in a beam under impact.*

Table 2. Comparison of spring-mass model with test results.

Specimen No.	Impact Velocity (m/s)	Test Results		Spring-Mass Model	
		Max. Force (N)	Duration (ms)	Max. Force (N)	Duration (ms)
7	0.75	1689	20.82	1518	21.48
8	0.97	2069	21.89	1963	21.48

not grow during impact. The flexural stiffness of the delaminated beam was computed by solving the static problem using offset beam finite elements. For the beam considered, the effect of delamination was to reduce the stiffness by about 20%. The expressions for maximum impact force and duration can be derived as [10]

$$F_0 = V_0 \sqrt{M_s K} \tag{10}$$

$$T = \pi \sqrt{M_s / K} \tag{11}$$

where M_s is the impact mass, V_0 is the impact velocity and K is the beam flexural stiffness. Comparison of spring-mass model predictions and experimental results are shown in Table 2, and the agreement is very good.

SUMMARY

A novel beam finite element with nodes offset to either top or bottom side has been developed to study the problem of delamination crack propagation in beam type composite specimens. These elements are used to model the sublaminates above and below the plane of delamination. The dynamic energy release rate is computed from the strain energy stored in the crack-tip springs that connect the undelaminated portions of the beam. The crack growth is simulated by breaking the crack-tip springs whenever the energy release rate exceeds a critical value. The model was evaluated by comparing with experimental results obtained by impacting beams containing implanted delaminations. The finite element model is able to predict crack growth history and final extent of delamination. The offset nodes and the spring connections are convenient in modeling dynamic fracture as node renumbering is avoided as the crack grows, and the procedure for computation of G is also very simple. This method can be used to evaluate impact damage tolerance of composite structures containing delaminations.

ACKNOWLEDGEMENTS

This research was partially supported by a DARPA grant to the University of Florida under the program Innovative Processing of Composites for Ultra High Temperature Applications, and by the state of Florida under the University of Florida Engineering Center of Excellence Program in New Materials.

APPENDIX

The non-zero coefficients of the (symmetric) stiffness matrix are: $k_{11} = 7\varkappa bA_{55}/3L$, $k_{12} = -5\varkappa bA_{55}/6$, $k_{14} = -8\varkappa bA_{55}/3L$, $k_{15} = \varkappa bA_{55}/3L$, $k_{16} = -\varkappa bA_{55}/6$, $k_{22} = (4bD_{11}/L) + L\varkappa bA_{55}/3$, $k_{23} = \pm bhA_{11}/2L$, $k_{24} = 2Lk_{15}$, $k_{25} = -k_{16}$, $k_{26} = -(4bD_{11}/L) + Lb\varkappa A_{55}/6$, $k_{27} = -k_{23}$, $k_{33} = bA_{11}/L$, $k_{36} = k_{27}$, $k_{37} = -k_{33}$, $k_{44} = -2k_{14}$, $k_{45} = k_{14}$, $k_{46} = -2k_{15}$, $k_{55} = k_{11}$, $k_{56} = -k_{12}$, $k_{66} = k_{22}$, $k_{67} = k_{23}$, $k_{77} = k_{33}$, where L, b, and h are element length, width, and thickness respectively, $\varkappa$ is the shear correction factor.

The non-zero coefficients of the (symmetric) mass matrix are: $M_{11} = 2m/15$, $M_{14} = m/15$, $M_{15} = -m/30$, $M_{22} = mh^2/9$, $M_{23} = \pm mh/6$, $M_{26} = M_{22}/2$, $M_{27} = M_{23}/2$, $M_{33} = m/3$, $M_{36} = M_{27}$, $M_{37} = m/6$, $M_{44} = 4M_{11}$, $M_{45} = M_{14}$, $M_{55} = M_{11}$, $M_{66} = M_{22}$, $M_{67} = M_{23}$, $M_{77} = m/3$, where m is the mass of the beam element.

REFERENCES

1. Freund, L. B. 1985. "The Mechanics of Dynamic Growth in Solids," *Fundamentals of Deformation and Fracture*, B. A. Bilby, K. J. Miller and J. R. Willis, eds., Cambridge: Cambridge University Press, pp. 163–185.
2. Grady, J. E. and C. T. Sun. 1986. "Dynamic Delamination Propagation in a Graphite/Epoxy Laminate," *Composite Materials: Fatigue and Fracture, ASTM STP 907*, pp. 5–31.
3. Kanninen, M. F. 1974. "A Dynamic Analysis of Unstable Crack Propagation and Arrest in the DCB Test Specimen," *International Journal of Fracture*, pp. 415–430.
4. Kanninen, M. F. and C. H. Popelar. 1985. *Advanced Fracture Mechanics*. New York: Oxford University Press.
5. Shmuely, M. 1977. "Analysis of Fast Fracture and Crack Arrest by Finite Differences," *International Journal of Fracture*, pp. 443–453.
6. Owen, D. R. J. and D. Shantaram. 1977. "Numerical Study of Dynamic Crack Growth by the Finite Element Method," *International Journal of Fracture*, pp. 821–837.
7. Farris, T. N. and J. F. Doyle. 1988. "Estimating Dynamic Stress Intensity Factors in a Lengthwise Cracked Beam Using Remote Data," *Engineering Science Prepring ESP25.88026*, Society of Engineering Sciences.
8. Sankar, B. V. 1991. "A Finite Element for Modeling Delaminations in Composite Beams," *Computers and Structures*, 38(2):239–246.
9. Sankar, B. V. and M. A. Pinheiro. 1990. "An Offset Beam Finite Element for Fracture Analysis of Delaminations," *AIAA 31st SDM Conference, Long Beach, CA, April 1990*, pp. 1227–1233.
10. Hu, S. 1990. "Dynamic Delamination Propagation in Composite Beams Under Impact," PhD dissertation, University of Florida, Gainesville, FL.
11. Cordell, T. M. and P. O. Sjoblom. 1986. "Low Velocity Impact Testing of Composites," *Proceedings of the American Society for Composites, First Technical Conference*. Lancaster, PA: Technomic Publishing Co., pp. 297–312.
12. Sankar, B. V. and C. T. Sun. 1985. "An Efficient Numerical Algorithm for Transverse Impact Problems," *Computers & Structures, Vol. 20*, pp. 1009–1012.